Proceedings of the 21st International Conference on Global Research and Education (Inter-Academia 2024)

Long-term Stability of Alignment of Biaxial Microelectromechanical System Accelerometers

S. Łuczak*, M. Zaczyk and H. Grzywacz

Faculty of Mechatronics, Institute of Micromechanics and Photonics, Warsaw University of Technology, św. A. Boboli 8, 02-525 Warsaw, Poland

Doi: 10.12693/APhysPolA.146.325 *e-mail: sergiusz.luczak@pw.edu.pl

The long-term stability of alignment precision of microelectromechanical system accelerometers was evaluated. Four commercial biaxial accelerometers (two ADXL 202E and two ADXL 203 accelerometers by Analog Devices Inc.) were tested over a period of 20 and 15 years, respectively. The experimental studies were performed using a custom computer-controlled test rig and employing gravitational acceleration as the reference. Considerable changes in the existing misalignments were observed. It was found that not only misalignments between the sensitive axes changed over time, but due to some micromovements within the mounting of the printed circuit board with the accelerometer chip, misalignments of the sensitive axes with respect to the mounting datum changed as well. Even though no bigger than 0.6°, the observed misalignments may considerably influence the accelerometer performance, especially in the case of tilt measurements. Some ways of increasing the considered long-term stability of printed circuit board mounting are proposed.

topics: stability, aging, microelectromechanical systems (MEMS), misalignment

1. Introduction

Even though quantified results regarding the aging of silicon are rarely published [1, 2], and some of such publications claim that the aging effects are rather insignificant [3–6], it is relatively easy to find contradicting statements [7, 8] and reports about aging phenomena clearly observed in *microelectromechanical system* (MEMS) devices [9–12], or even in MEMS accelerometers specifically [13–15]. However, according to our best knowledge, no research was devoted to the long-term stability of alignments of the sensitive axes of MEMS accelerometers, both in the sense of mutual misalignments and in the sense of misalignments of the sensitive axes with respect to the mounting datum of the housing of the device that contains the MEMS accelerometer. While analyzing aging phenomena in the case of biaxial and triaxial MEMS accelerometers, reported in [16–17], we found that not only the off-sets and the scale factors associated with particular sensitive axes changed over the long term, but also their misalignments. As stated in [18], alignment precision is a crucial issue pertaining to the application of MEMS accelerometers, especially with respect to their calibration accuracy. It is an important statement, because one of the ways of compensating for errors due to aging is cyclic repetition of the calibration process [11, 17, 19]. Moreover, precise alignment is an important issue pertaining to the determination of tilt [20], especially when high accuracy of the measurements is expected. Results of related experimental studies reported in [21, 22] clearly prove the above statement, reporting respective errors due to misalignment up to a few degrees arc. Another untypical feature of the presented study, besides dealing with the long-term stability of alignment precision, is the fact that we report on the effects of purely natural aging, whereas the majority of similar research works involves accelerated tests, e.g., [14, 23, 24], when a MEMS device is subjected, over a relatively short period of time, to vibration, high or low temperature, thermal and moisture cycling, or harsh electrical loading, as reported in [14, 25, 26]. However, some publications question the reliability of such accelerated tests performed on MEMS devices [27], whereas others point to the stability of even theoretical models compensating for misalignments in attitude control [28]. So, to conclude, it may be stated that natural aging is a more reliable method of evaluating long-term stability. Throughout the whole time of the study (2003–2024), the tested accelerometers were stored in laboratory rooms, with the ambient temperature kept in the range of 15–40°C. Results concerning significant aging effects related to the offsets and the scale factors of particular

sensitive axes of the tested accelerometers were presented by the authors in [16]. In this paper, we discuss aging effects related to alignment precision, determined on the basis of the same experimental results.

2. Materials and methods

2.1. Experimental studies

One of the typical applications of MEMS accelerometers is tilt measurements [29], where the components of gravitational acceleration (being one of the most stable and accurate external reference sources) are the measured quantities. Regarding low-g MEMS accelerometers, the magnitude of gravitational acceleration is well-adjusted to their measurement range. To evaluate the considered effects of aging observed in alignments of MEMS accelerometers, it was decided to repeat a calibration procedure 90 times over a long-term period. The interval between performing the calibration procedures was not constant — sometimes it was a few days, sometimes a few months. The calibration consisted of changing the position of the tested accelerometer with respect to the gravity vector and then recording a series of its output signals. The position was changed only within one of two vertical planes at a time. As the accelerometers were arranged in such a way as to create a triaxial acceleration sensor (corresponding to a dual-axis tilt sensor), the plane of rotation was either a pitch plane or a vertical roll plane (with no pitch involved, see Fig. 1).

Two kinds of dual-axis MEMS accelerometers by Analog Devices Inc. were tested: (i) ADXL 202E [30] — manufactured no later than 2002, and (ii) ADXL 203 [31] — manufactured no later than 2005. The accelerometers (two pieces of each kind) are presented in Fig. 2a (202E with sensitive axes G, R, W, B) and in Fig. 2b (203 with sensitive axes O, P, S, V).

In the experiments, two pieces of each dual-axis accelerometer were used at the same time. Thus, components of the gravitational acceleration were measured in x, y, z axes, yet in the case of ADXL 202E, there were two x axes, whereas for ADXL 203, two y axes. Referring to the initial position of the accelerometers while fixed in the test rig, axes W (white), R (red), V (violet) correspond to the x axis, axes B (blue), S (silver), P (pink) to the y axis, and axes G (green), O (orange) to z axis. The calibration made it possible to determine the parameters of the analog output signals of the accelerometers. The signals can be represented in the following formulas. In the case of applying pitch angle α [16],

$$U_x = a_x + b_x \sin(\alpha + c_x), \tag{1}$$

$$U_z = a_{z\alpha} + b_{z\alpha} \cos(\alpha + c_{z\alpha}), \tag{2}$$

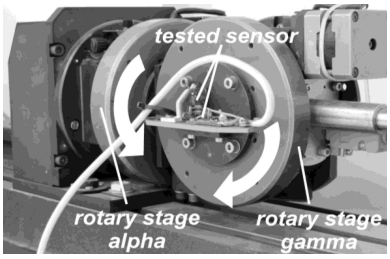

Fig. 1. Calibration by applying pitch and roll angle (the tested sensor is presented in Fig. 2a).

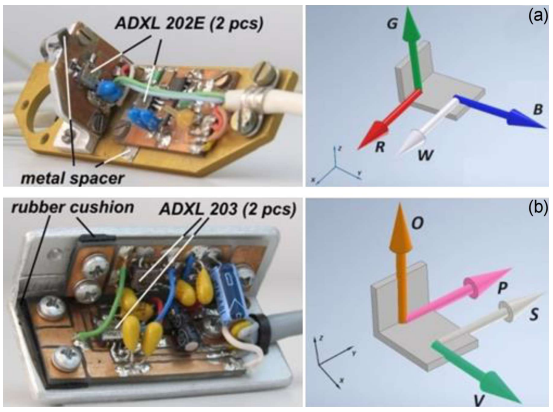

Fig. 2. The tested accelerometers and sensitive axes: (a) ADXL 202E, (b) ADXL 203.

and in the case of applying roll angle γ,

$$U_y = a_y + b_y \sin(\gamma + c_y), \tag{3}$$

$$U_z = a_{z\gamma} + b_{z\gamma} \cos(\gamma + c_{z\gamma}), \tag{4}$$

where U_x, U_y, U_z are output voltage assigned to x, y, z axis [V], respectively; a_x, a_y, a_z — offset of the output voltage assigned to U_x, U_y, U_z [V], respectively; b_x, b_y, b_z — scale factor of the output voltage assigned to U_x, U_y, U_z [Vg^{-1}], respectively; $c_x, c_y, c_{z\alpha}, c_{z\gamma}$ — geometrical phase shift of the output voltage assigned to U_x, U_y, U_z [deg], respectively; α — pitch applied by means of the test rig [deg]; γ — roll applied by means of the test rig [deg]. According to Fig. 1, $x \Leftrightarrow W, R, V$; $y \Leftrightarrow B, S, O$; $z \Leftrightarrow G, O$. Whereas approximately the offset and the scale factor of the output voltage assigned to U_z is the same, i.e.,

$$a_{z\alpha} \approx a_{z\gamma}, \tag{5}$$

$$b_{z\alpha} \approx b_{z\gamma}. \tag{6}$$

It should be noted that the geometrical phase shifts are generally different, as related to alignment precision during the assembly, i.e.,

$$c_{z\alpha} \neq c_{z\gamma}. \tag{7}$$

The calibration process was realized by means of the presented test rig, whose main elements were two rotary stages, applying pitch and roll angles with precision of at least $\pm 0.02^\circ$ (see Fig. 1), controlled by a computer with a data acquisition

module (Advantech PCL-818L/PCI-1716) installed for reading the analog output voltages of accelerometers. The whole test rig has been described by the authors in [16]. In the case of ADXL 202E, the first calibration was performed in June 2003, whereas in the case of ADXL 203, it was in December 2008. The last calibrations took place in June 2012. Then, in January 2024, all four accelerometers were calibrated again — each twice (applying pitch and roll). Equipment with similar mechanical structure can be easily found in relevant publications, e.g., in [32]. The employed test rig features high kinematic precision, however it operates in a controllable manner only under static conditions. In experimental studies, when dynamic operation would be necessary, more sophisticated equipment must be used, like the one presented in [33]. A methodology employed for performing the experimental studies by means of the test rig, including a fast alignment procedure developed for that purpose [34], was the following. The computer activated a respective rotary stage (the rotation axis of the active stage was always horizontal during the tests), set its desired position, and then recorded a series of 30 output voltages of the tested accelerometers. Each test consisted of rotating the accelerometers over the full range (360°) of pitch or roll, respectively. In most of the cases, the angular positions were changed with a step of 1° or 5°. At each angular position, when the rotary stage had already reached the desired position and was immobile, the output voltages were sampled 30 times and their values recorded in the computer memory. So, each calibration consisted of 10800 or 2160 records. In the case of applying the roll angle, each calibration procedure was preceded by calibrating the accelerometers with respect to pitch in order to precisely find the zero-pitch angle and only then apply pure roll angle in the next step. In order to determine parameters $a_{x\ldots z}, b_{x\ldots z}, c_{x\ldots z}$ of (1)–(4), the recorded data were processed by means of statistical software (Statgraphics), employing a nonlinear regression model consistent with (1)–(4). It was accepted that subscripts of the offset $a_{x\ldots z}$ and the scale factor $b_{x\ldots z}$ are consistent with the labels of the sensitivity axes of the accelerometers introduced in Fig. 2. Occasionally, due to lack of time while testing the accelerometers, not all output signals of the accelerometers were tested in each study. The presented data consist of 32 calibration procedures for ADXL 202E and 58 for ADXL 203 (this can be expressed as ca. 96 or 174 h of operation, respectively). Not only the geometrical phase shifts specified in (7) are significantly different, but the same also concerns the phase shifts ci introduced in (1)–(4) for each experiment, since their random value is dependent on particular conditions pertaining to each mounting of the accelerometers in the test rig (mutual position, applied fastening torque, leveling of the rotary stages). So, in order to verify if the real changes took place in the alignment of the accelerometer sensitive axis with respect to its housing (which includes both alignment of the sensitive axis with respect to the *printed circuit board* (PCB) and alignment of the PCB with respect to the housing), only the difference of appropriate phase shifts related to a particular calibration procedure should be considered.

TABLE I

Misalignment changes due to aging (ADXL 202E, ADXL 203); Max — maximal value; Min — maximal value; Range — absolute difference between 'Max' and 'Min'.

Sensor	Misalignment	Cartesian axes	Max	Min	Range
202E	$\eta_1 = c_W - c_{G\alpha}$	x, z	0.41°	0.01°	0.40°
202E	$\eta_2 = c_B - c_{G\gamma}$	y, z	0.30°	0°	0.30°
202E	$\eta_3 = c_R - c_{G\alpha}$	x, z	0.55°	0.08°	0.47°
202E	$\eta_4 = c_W - c_R$	x, x	0.12°	−0.18°	0.30°
203	$\eta_5 = c_V - c_{O\alpha}$	x, z	0.41°	0.05°	0.36°
203	$\eta_6 = c_S - c_{O\gamma}$	y, z	0.19°	−0.07°	0.26°
203	$\eta_7 = c_P - c_O$	y, z	0.38°	0.07°	0.31°
203	$\eta_8 = c_S - c_P$	y, y	0.05°	−0.27°	0.33°

2.2. Experimental results

Two kinds of changes had to be analyzed: first, changes related to the external mounting of the PCB, and second, internal changes within the accelerometer itself. In the case of the presented results, the following misalignments η (as defined in Table I) were considered:

- when applying pitch angle: η_1, η_3, η_4, η_5,
- when applying roll angle: η_2, η_6, η_7, η_8.

Since in the case of both types of accelerometers, we tested dual-axis sensors by applying pitch or roll angle, we can determine two errors of perpendicularity between the sensitive axes *R*–*G* and *P*–*O* — one error for each type of sensor. These are, respectively, η_3 and η_7. Errors of perpendicularity between the sensitive axes *W*–*B* and *S*–*V* could not be determined because the tested accelerometers were not rotated about the *G* or *O* axis, respectively. The extreme values of the detected misalignments, as well as the range of their variations, are listed in Table I (the subscripts are consistent with the arrangement in Fig. 2.).

Assuming an ideal alignment, the two sensitive axes of each accelerometer would be perfectly perpendicular (no inherent misalignment), and the respective axes of the two accelerometers would be perpendicular as well (no mounting misalignment). The observed changes are of a rather random character. Two issues are difficult to explain. First, even though only the PCBs with ADXL 202E were realigned a few times over the testing time, the range

of the observed changes was similar compared to ADXL 203. Second, even though the mounting of the PCB with ADXL 203 consisted of some elements made of rubber (which is prone to adverse material changes over the lapse of time due to many factors: temperature, exposure to sunlight, etc.), whereas the mounting of the PCBs with ADXL 202E consisted of more stable metal elements (see Fig. 2a), no significant difference in misalignments can be observed. As aforementioned, values of η_3 and η_7 are errors of perpendicularity (inherent misalignment) between sensitive axes of a single accelerometer (in our case, axes R and G of ADXL 202E and axes P and O of ADXL 203 — see Fig. 2a). One can expect that the values should be rather constant and smaller, as the relevant data sheets declare their magnitudes as 0.01° or 0.1° [30–31], which in the first case is a clearly underestimated value, as our own experiments proved. However, since the obtained results are much higher than 0.1°, these values should be regarded as rather overestimated. In light of the above, the other misalignments also seem to be overestimated. Nevertheless, it can be firmly stated that the misalignments did not change more than 0.6° within the period of 20 years.

3. Discussion

Mounting of the accelerometer chips should be considered an important issue. For example, additional gluing of the chip to the PCB (strengthening the soldered joints) may prevent limitation of the bandwidth in the case when the accelerometers operate under dynamic conditions. However, as the presented results prove, careful attention must be paid to the mounting of the whole PCB with the accelerometer chip, if related effects of aging are to be limited. So, the PCB should be firmly fixed to the housing. It is notable that the accelerometers were aligned in various ways. In the case of ADXL 202E, metal pads were used, whereas in the case of ADXL 203, cushions made of rubber were used (see Fig. 2b). As the results reveal, the application of the rubber elements did not result in bigger misalignments, even though such effect might be expected. Nevertheless, rubber elements should be avoided if a device is to have a good performance over a longer period of time, unless a calibration is cyclically repeated, which allows the misalignments to be compensated for. As aforementioned, misalignments affect the calibration accuracy of MEMS accelerometers [18]. Besides, the misalignment of a sensitive axis may result in an apparent nonlinearity of the accelerometer characteristic [35]. However, in the case of the discussed experiments, these general statements must be considered more precisely. First, it may be the case that the calibration takes place within a plane that is not vertical. Let us consider applying the roll angle γ (at a pitch α of nonzero value) by means of the test rig (the same applies to the pitch α accordingly). In such case, the respective accelerometer output measures angle β instead of γ, where

$$\beta = \sin^{-1}\big(\sin(\gamma)\cos(\alpha)\big). \tag{8}$$

Then, the resultant error e can be determined as

$$e = |\beta - \gamma| = \left|\sin^{-1}\big(\sin(\gamma)\cos(\alpha)\big) - \gamma\right|. \tag{9}$$

For small pitch angles (that can be evaluated here at ca. 0.1°), the maximal value of this error is the same as the value of the pitch. Such error could result in an apparent decrease in the respective scale factor. However, the decrease would be insignificant, especially because of the fact that except for roll angles of ca. 90° (and multiples of 90°), the discussed error is very small. Second, it should be noted that one of the possible options of determining a misalignment of each sensitive axis of an accelerometer is to represent it as two component angles (contained within two perpendicular planes), as proposed, e.g., in [36–38] (in the case of rotations of the accelerometer about one axis, usually only one component angle is provided [39–40]), whereas other options are to represent misalignments as nonorthogonalities between the sensitive axes and the frame [41] or to use attitude quaternions instead [42]. One of the component angles (contained within the plane of rotation) is included in (1)–(4) — it is the geometric phase shift, and has no significant influence whatsoever. The other component (contained within a horizontal plane) is more important here. Referring to the roll angle again, the respective component of the gravitational acceleration measured by the accelerometer in such a case can be determined as

$$g_y = g\sin(\gamma)\cos(\alpha). \tag{10}$$

As it results from the authors' own experiments, a typical misalignment of this kind can be evaluated at ca. 1°. Then, the resultant error is less than 0.016%, so it can be also neglected. In order to prove it experimentally, some additional tests were carried out, where the misalignments of ca. 1° were introduced purposefully. However, no significant differences in values of the offset, the scale factor, and the phase shift were observed [43]. Concluding, it can be stated that the existing misalignments (being also subject to changes due to aging) could not have influenced the obtained results significantly.

4. Conclusions

The presented study is related to both aging phenomena in the silicon structure of the accelerometer and the mechanical mounting of the PCB. A relatively large decrease in accuracy due to natural aging phenomena was determined in terms of changes in the mounting technique, discovering that it is important not only with respect to attaching a MEMS accelerometer to its PCB, but also with respect to

fixing the PCB to its housing. In the case of the mechanical mountings of the PCBs, changes in the existing misalignments no bigger than 0.6° were observed. Therefore, such errors cannot be overlooked in the case of applying MEMS accelerometers where high precision is required within a longer period of time. Moreover, there are a few other factors that most probably will considerably intensify the aging effects. These are: mechanical overloads (including high-g shocks) of the accelerometer both while operated and while stored (the tested accelerometers were not overloaded within their whole life), a scatter of various operational parameters within the production batch (in the case of the tested accelerometers it is a significant factor, as reported in the relevant datasheets [30, 31]), and material fatigue of mechanical elements of the accelerometer. So, it is rather certain that the values of errors related to aging phenomena will be in many cases bigger than the reported ones. In conclusion, even though the observed effects are rather overestimated, in the case of using similar MEMS accelerometers under more harsh conditions (frequent operation — resulting in material fatigue, mechanical overloads/shocks, wide range of changes in the ambient temperature), even bigger changes in their operational parameters should be taken into account. As the observed degradation of long-term stability of the alignment precision, and the offset and scale factors as well [16], are of relatively large values, it is advantageous to repeatedly calibrate the operated accelerometer, however, the employed calibration procedure is to regard corrections for the misalignment angles assigned to each sensitive axis of the accelerometer. Measurement systems, like, e.g., 3DM-GX3-25 by MicroStrain Inc., that can be calibrated even while operated [44], seem to be a very advantageous solution. Then, the related errors can be to some extent compensated for, and thus, the considered long-term instability reported in the paper may be neglected. Due to the low precision of the proposed method of determining accelerometer misalignments on the basis of phase shifts, a new study is planned, where a different technique (i.e., method and instrumentation) will be used — a special manually driven precise optical dividing head with only one axis of rotation equipped with additional unit for direct physical determination of misalignments (both internal and external) as well as a special holder for the tested accelerometers with three perpendicular reference surfaces.

Acknowledgments

This research was funded by the Scientific Council for the Discipline of Automatic Control, Electronics, Electrical Engineering and Space Technologies at the Warsaw University of Technology, grant number 504/04873/1143/43.022301.

A considerable part of the data used for processing the final results presented in the paper was obtained by the students of the Faculty of Mechatronics, Warsaw University of Technology, specializing in Micromechanics, while realizing experimental works during a laboratory class "Studies of tilt sensors" within academic years 2008/09–2012/13.

References

[1] A. Neels, A. Dommann, A. Schifferle, O. Papes, E. Mazza, *Microelectron. Reliab.* **48**, 1245 (2008).

[2] A. Neels, G. Bourban, H. Shea, A. Schifferle, E. Mazza, A. Dommann, *Proc. Chem.* **1**, 820 (2009).

[3] F. Schneider, T. Fellner, J. Wilde, U. Wallrabe, *J. Micromech. Microeng.* **18**, 065008 (2008).

[4] S. Habibi, S.J. Cooper, J.-M. Stauffer, B. Dutoit, in: *IEEE/ION Position, Location and Navigation Symposium, Monterey (CA)*, IEEE, 2008, p. 232.

[5] A. Ya'akobovitz, S. Krylov, *IEEE Sens. J.* **10**, 1311 (2010).

[6] Y. Yang, E.J. Ng, P.M. Polunin, Y. Chen, I.B. Flader, S.W. Shaw, M.I. Dykman, T.W. Kenny, *J. Micromech. Microeng.* **25**, 859 (2016).

[7] Y. Xing, T. Yu, H. Yan C. Yue, J. Zhao, M. Hu, *IEEE Sensors J.* **23**, 21327 (2023).

[8] A. Yang, P. Wang, H. Yang, *IEEE Sensors J.* **21**, 24274 (2021).

[9] V. Mulloni, M. Barbato, G. Meneghesso, *J. Micromech. Microeng.* **26**, 074004 (2016).

[10] C.H. He, Y.P. Wang, Q.W. Huang, Q.C. Zhao, Z.C. Yang, D.C. Zhang, in: *Proc. 2017 19th Int. Conf. Solid-State Sensors, Actuators and Microsystems (TRANSDUCERS), Kaohsiung, Taiwan*, IEEE, 2017.

[11] J. Zhang, Y. Wu, Q. Liu, F. Gu, X. Mao, M. Li, *Micromachines* **6**, 554 (2015).

[12] M. Barbato, A. Cester, G. Meneghesso, *IEEE Trans. Electron Devices* **63**, 3620 (2016).

[13] X. Xiong, Y.-L. Wu, W.-B. Jone, in: *IEEE Int. Symp. on Defect and Fault Tolerance of VLSI Systems, Boston (MA)*, IEEE, 2008, p. 314.

[14] A.S. Önen, Y. Günhan, in: *2018 IEEE/ION Position, Location and Navigation Symposium (PLANS), Monterey (CA)*, IEEE, 2018, p. 546.

[15] P. Peng, W. Zhou, L. Li, J. He, B. Peng, H. Yu, *IEEE Sens. J.* **23**, 202 (2023).

[16] S. Łuczak, J. Wierciak, W. Credo, *IEEE Sens. J.* **21**, 1305 (2021).

[17] S. Łuczak, M. Zams, K. Bagiński, *J. Sens.* **2019**, 5184907 (2019).

[18] Z. Syed, P. Aggarwal, C. Goodall, X. Niu, N. El-Sheimy, *Meas. Sci. Technol.* **18**, 1897 (2007).

[19] W.S. de Ajúro Rocha, J.C.G. Rodrigues, A.A.A.E. de Queiroz, A.A.A. de Queiroz, *IEEE Sens. J.* **20**, 155 (2020).

[20] S. Łuczak, *Int. J. Precis. Eng. Manuf.* **15**, 2012 (2014).

[21] B. Fan, Q. Li, T. Tan, P. Kang, P.B. Shull, *IEEE Sens. J.* **22**, 2543 (2022).

[22] S. Łuczak, in: *Mechatronics 2013. Recent Technological and Scientific Advances*, Eds. T. Brezina, R. Jabłoński, Springer International Publishing, Cham 2014 p. 393.

[23] J. Segovia-Fernandez, Y. Suzuki, M. Chowdhury, J. Rojas, E.T.-T. Yen, in: *Proc. Joint Conf. Eur. Frequency Time Forum IEEE Int. Frequency Control Symp. (EFTF/IFCS)*, 2022, p. 1.

[24] J. Segovia-Fernandez, E. Tuncer, S. Chang, and E.T.-T. Yen, in: *Proc. Joint Conf. Eur. Frequency Time Forum IEEE Int. Frequency Control Symp. (EFTF/IFCS)*, 2022 p. 1.

[25] J. Dhennin, D. Lellouchi, F. Pressecq, in: *Proc. 2015 Symp. Design, Test, Integration and Packaging of MEMS/MOEMS (DTIP), Montpellier, France*, 2015, p. 1.

[26] K. Krupa, C. Gorecki, R. Jóźwicki, M. Józwik, A. Andrei, *Sens. Actuators A* **171**, 306 (2011).

[27] H.R. Shea, in: *Proc. SPIE, Reliability, Packaging, Testing, and Characterization of MEMS/MOEMS V*, Vol. 6111, 2006, p. 61110A.

[28] L. Qian, F. Qin, K. Li, T. Zhu, *IEEE Sens. J.* **23**, 16968 (2023).

[29] J.S. Wilson, *Sensor Technology Handbook*, Newnes, Burlington (MA) 2005, p. 396.

[30] Analog Devices, Data Sheet no. ADXL103/ADXL203, Norwood (MA) 2004.

[31] Analog Devices, Data Sheet no. ADXL202E*, Norwood (MA) 2000.

[32] S. Yun, D. Jeong, S. Wang, C. Je, M. Lee, G. Hwang, C. Choi, J. Lee, *J. Micromech. Microeng.* **19**, 035025 (2009).

[33] C. Acar, A. Shkel, *J. Micromech. Microeng.* **18**, 634 (2003).

[34] S. Łuczak, in: *Advanced Mechatronics Solutions*, Eds. R. Jabłoński, T. Brezina, Springer International Publishing, Switzerland 2016, p. 481.

[35] MEMSIC, Application Note no. 5/12/03, #AN-00MX-014, North Andover (MA) 2005.

[36] M. Šipoš, P. Pačes, J. Roháč, P. Nováček, *IEEE Sens. J.* **12**, 1157 (2012).

[37] X. Ru, N. Gu, H. Shang, H. Zhang, *Micromachines* **2022**, 879, (2022).

[38] S. Łuczak, in: *Recent Advances in Mechatronics*, Eds. R. Jabłoński, M. Turkowski, R. Szewczyk, Springer-Verlag, Berlin 2007, p. 511.

[39] X. Dong, X. Huang, G. Du, Q. Huang, Y. Huang, Y. Huang, P. Lai, *Micromachines* **2022**, 62, (2022).

[40] S. Łuczak, in: *Mechatronics. Recent Technological and Scientific Advances*, Eds. R. Jabloński, T. Brezina, Springer-Verlag, Berlin 2012, p. 705.

[41] G. Zhao, M. Tan, X. Wang, W. Liang, S. Gao, Z. Chen, *Micromachines* **2023**, 697 (2023).

[42] M. Liu, Y. Cai, L. Zhang, Y. Wang, *Micromachines* **2021**, 1373, (2021).

[43] S. Łuczak, *IEEE Sens. J.* **15**, 3492 (2015).

[44] MicroStrain, Technical Note no. TN-I0029, 2012.